2112 *Journal of Mechanical Science and Technology 〈KSME I. J.〉 〈Special Edition〉 Vol. 19, No. 11, pp. 2112~2121, 2005*

A Study on the Effect of Pattern Pitch on Deformation Behaviors for Surface Patterning by Using Nano-indenter

Sung Won Youn, Hyun Il Kim
Department of Mechanical and Precision Engineering, Pusan National University, JangJung-dong, KumJung-gu, Busan, Korea
Chung Gil Kang*
School of Mechanical Engineering, Pusan National University, JangJung-dong, KumJung-gu, Busan, Korea

Nanoprobe-based lithography techniques have attracted tremendous interst. However, most of these techniques have the several technical problems still to be resolved such as low throughput, reproducibility, extensive processing time and tip-wear problem. We considered that a patterning process with a multi-array tip can be a solution. The purpose of this study is to build up the database in order to design a multi-array tip for patterning. In this study, the effects of tip-geometry factors (indenter shape and tip radius) and process parameters (pattern pitch and normal load) on the deformation behaviors and etching chracteristics of hard-brittle materials (Pyrex 7740 glass and silicon) were investigated by using both experiment and finite element analysis. The results of the investigation will be applied to the design of the multi-array tip for patterning.

Key Words : Lithography, Nanoscratch Test, Silicon, Borosilicate, Wet Etching

1. Introduction

Nanoprobe-based lithography techniques have attracted tremendous interest due to their operational versatility, low costs for initial facilities and manufacture, simplicity of process, and material selectivity. As examples of scanning probe lithography tools, SPM (atomic force microscopy (AFM) and scanning tunneling microscopy (STM)) and Nanoindenter can be enumerated (Ashida et al., 2001 ; Morita, 2001 ; Miyake and Kim, 2002 ; Miyake and Kim, 2001 ; Chang et al., 2003 ; Chung et al., 2004). The nanoindenter and SPM have already been used for nanofabrication such as nanolithography, nanowriting, and nanopatterning. SPM methods are based on the local modification of surfaces or thin overlayers by oxidation, depasivation, exposure, force, deposition, or etching. Because of the very short range nature of the tip-sample interaction, STM sample modifications are usually restricted to the outermost layers of the surface, and in many cases the process has to be carried out under special environmental conditions.

One of the most recent approaches is based on using an AFM equipped with a monocrystalline diamond tip to directly mechanically scratch a surface. This has been used to create nanostructures (indents and grooves) directly on a silicon surface or for indenting and scratching through an oxide covered Si(100) surface (Ashida et al., 2001 ; Morita, 2001 ; Miyake and Kim, 2002 ; Miyake and Kim, 2001 ; Chang et al., 2003). It is well known that the mode of machining hard-brittle materials such as silicon and glass is generally classified as ductile and brittle. In the ductile-regime machining process, the width and

* Corresponding Author,
E-mail : cgkang@pusan.ac.kr
TEL : +82-51-510-2335; **FAX** : +82-51-512-1722
School of Mechanical Engineering, Pusan National University, JangJung-dong, KumJung-gu, Busan, Korea. (Manuscript **Received** January 25, 2005; **Revised** May 13, 2005)

Copyright (C) 2005 NuriMedia Co., Ltd.

depth of the machined groove are determined by the elastic-plastic deformation characteristics of a materials as well as the geometry of the cutting tip. For example, the elastic recovery of materials can be a problem, which results in a groove with a low aspect ratio. Therefore, it is important to predict the elastic-plastic deformation behaviors of hard-brittle materials in order to control the width and depth of the cut groove. In addition, in case of pattern fabrication, a pattern pitch is important process parameters because the quality of cut groove can be influenced by the residual stress field and the pile-up of adjacent groove.

Probe-based lithography techniques face several technical problems still to be resolved such as low throughput, reproducibility, extensive processing time and tip-wear problem. We considered that a patterning process with a multi-array tip can be a solution.

With this motivation, in this study, the effects of tip-geometry factors (indenter shape and tip radius) and process parameters (pattern pitch and normal load) on the deformation behaviors and etching chracteristics of hard-brittle materials (Pyrex 7740 glass and silicon) were investigated by using both experiment and finite element anaysis. The results of the investigation will be applied to the design of the multi-array tip for patterning.

2. FEM Modeling and Experiments

2.1 Single tip

Three types of rigid indenters (conical α=65°, Berkovich β=70.3°, and spherical R=2 μm) (MTS Systems Corporation, 2002) were used in order to define models, as shown in Fig. 1. The finite element mesh is shown in Fig. 2. Since very small indentations were being simulated, the meshes near the indenter needed to be very fine to be able to describe the deformation and stress gradients associated with indentation with sufficient accuracy. Thus, extremely fine mesh sizes of 1-10 nm were used under the indenter. The specimens were modeled with 1281 4-node axi-symetic elements (CAX4R element type (Hibbitt, Karlsson and Sorenson, 2001)). The thickness and width of the specimens were 2 μm and 6 μm, respectively. The nodes along the axis of rotation can move only along the y axis, and all the nodes on the bottom of the mesh were fixed. Contact between two contacting surfaces, in this case the indenter surface and the specimen surface, was assumed. The friction coefficient between the tip

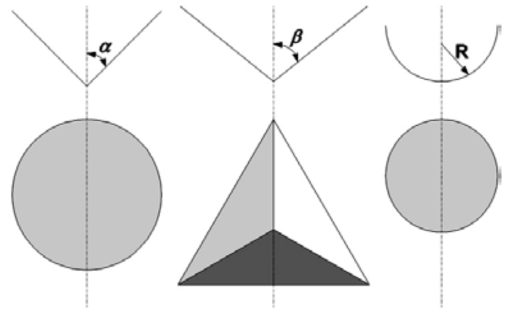

Fig. 1 Shape of Indenters

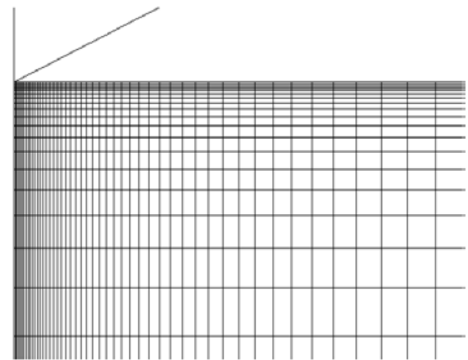

(a) Two-dimensional model of nanoindentation process

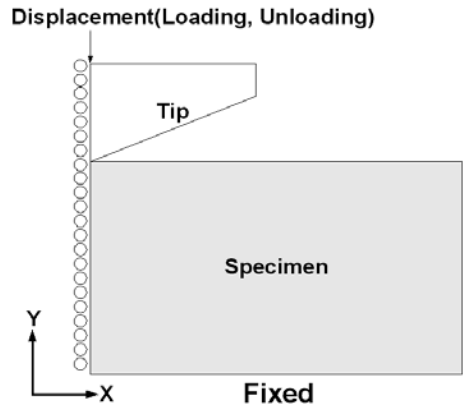

(b) Boundary conditions

Fig. 2 FEM model and boundary condition

Copyright (C) 2005 NuriMedia Co., Ltd.

and the specimen surface was assumed to be 1. The indentation procedure was simulated in two alternating steps, loading and unloading. During loading, the rigid surface or the modeled tip moves along the y direction and penetrates the specimen up to the maximum depth. During unloading, the tip returns to the initial position. Since strain hardening was not considered in this study, all specimens were assumed to be isotropic, linear elastic, perfectly plastic materials. Generally, amorphous materials are not expected to show hardening behavior. For isotropic materials, elastic deformation ceases and yielding commences when the von Mises yield criterion is satisfied. To predict the elastic recovery and pile-up of hard-brittle materials (amorphous silicon and Pyrex 7740 glass) that occur during a nanoscale indentation process, simulations were performed for various tip radii (40, 100, and 200 nm) and tip geometries (conical, Berkovich, and spherical) using the large-strain elastoplastic feature of the ABAQUS finite element code. The materials used in the calculations are given in Table 1. The yield strength and Poisson's ratio are the values of bulk material (Lu and Bogy, 1995). In order to measure the elastic modulus and the hardness of the materials, a depth-sensing indentation experiments were performed on a Nanoindenter® XP using the continuous stiffness measurement (CSM) method. This method measures hardness and elastic modulus as a continuous function of depth into the specimen. For the experiments in this study, the CSM imposed a 1 nm oscillation at 45 Hz on the loading curve. A detailed description of the theory behind this procedure was given by Oliver and Pharr (Oliver and Pharr, 1992).

Table 1 Elastic and plastic properties of silicon and Pyrex glass

Materials	Young's modulus (GPa)	Yield strength (Gpa)	Poisson's ratio
Silicon	127	4.4	0.278
Pyrex 7740 glass	63	0.063	0.17

2.2 Multi-array tip

Rigid conical indenters (α=65°) was used in order to define model, as shown in Fig. 3. The specimens were modeled with 5151 4-node plain strain elements (CPE4R element type (Hibbitt, Karlsson and Sorenson, 2001)). The thickness and width of the specimens were 10 μm and 20 μm, respectively.

2.3 Patterning by the nanoscratch with wet etching

All ductile-regime nano/micro machining experiments were performed using the constant load scratch (CLS) option of the Nanoindenter® XP (MTS, USA). Pyrex 7740 glass and n-type Si(100) wafers were used for experiments. They were initially cleaned only with distilled water. The surface roughnesses Ra of both specimens' surface were less than 5 nm. The diamond Berkovich having a tip radius of about 40 nm was used for the experiments. Prior to experiment, five indents were made in pure Al to clean up the tip, and then two indents were made in standard

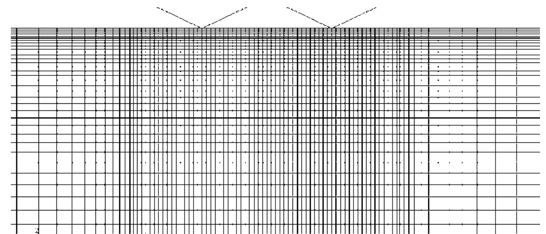

Fig. 3 Multi-tip nanoindentation process two-dimensional model

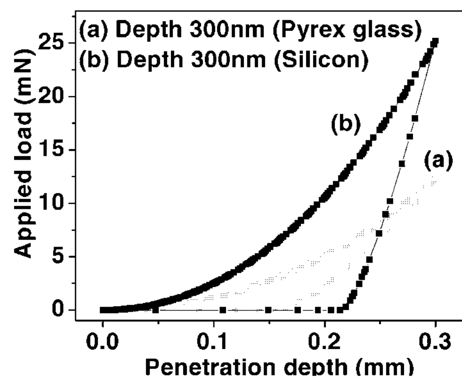

Fig. 4 Load-displacement curves for each materials

Copyright (C) 2005 NuriMedia Co., Ltd.

sample, fused silica, to evaluate the condition of tip. For the observation of the specimens, an XE-100 AFM system (PSIA, South Korea) was used. The CLS experiments and AFM observation were performed under atmospheric conditions of room temperature (20-21℃) with relative humidity ranging between 41% and 45%. Unless otherwise indicated, the normal load (L_n) and scratch velocity (S_s) conditions were 5 mN and 10 μm/s, respectively. An ultrasonic wave washer was used for the cleaning and wet etching processes. In case of Si(100) specimen, the CLS experiments were performed along the (Ashida et al., 2001 ; Oliver and Pharr, 1992) direction, which material is usually used in high-precision machining, since the characteristics of the fracture depend on the crystallographic directions on the Si(100) wafer (Blacley and Scattergood, 1990 ; Shibata et al., 1996). After the CLS experiments, Si(100) specimens were dipped in a Teflon beaker containing 20wt% KOH solution.

3. Results and Discussion

3.1 Difference between Pyrex 7740 and silicon

An indentation simulation for amorphous silicon and Pyrex 7740 glass, with maximum depths of 300 nm, was performed. A perfectly sharp Berkovich indenter was used for the simulation. We explored two distinct phenomena of silicon and amorphous borosilicate and attributed the different results to different intrinsic property (elastic modulus (E)/plastic strength (Y)) of two kinds of materials. In order to realize how impact on nano-scratching of E/Y and surface morphology, some other factors such as crystal orientation and crystal structure was excluded. The calculated load-displacements are shown in Fig. 5, which data will be used to determine the forming load in the process of fabricating the pit array to the desired depth. The elastic recovery of the amorphous silicon and the Pyrex 7740 glass was about 26% and 50% of the maximum penetration depth, respectively. It was reported that the degree of the elastic recovery increases with decreasing the value of elastic modulus over the plastic strength (E/Y) (Fischer-

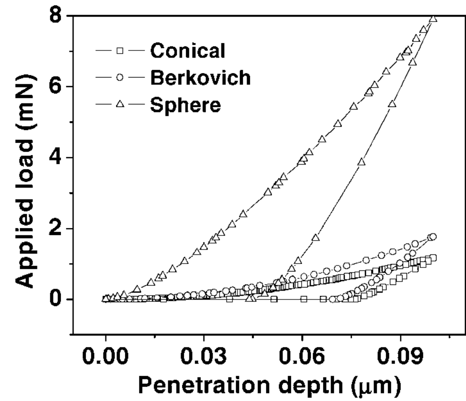

Fig. 5 Load-Displacement curves on silicon with different tip shape

Cripps, 2002). The E/Y values of the silicon and the Pyrex 7740 glass were 23 and 10.3, respectively. The E/Y value is of considerable interest since it may characterize the conditions under which a general elastic-plastic material exceeds its elastic limit and undergoes plastic deformation.

3.2 Effects of the indenter geometry and the tip radius (single tip)

Load-displacement curves using different indenters are shown in Fig. 5. For a given indentation depth, the applied load was the lowest in the case of the conical indenter. In addition, the results for the conical indenter showed the smallest elastic recovery. The elastic recovery for the conical, Berkovich, and spherical shapes was 26%, 32%, and 53%, respectively. This indicates that the cone-shaped indenter is the best for fabricating a hyperfine pit array. In the machining of nonlinear patterns, such as a pit array, the conical indenter can be a solution, but it has a blunter tip than the Berkovich indenter. The best tip radius that can be commercially achieved for a diamond conical indenter is about 500 nm. For line-pattern fabrication, a Berkovich or cube-corner-pyramid indenter (tip radius of min. 40 nm) is desirable because it produces plasticity at very low loads, has good manufactured quality, and minimizes the influence of friction. The stress-distributions on the materials after the loading and unloading steps of a procedure are shown in Fig. 6. The vertical stress distribution induced by

Copyright (C) 2005 NuriMedia Co., Ltd.

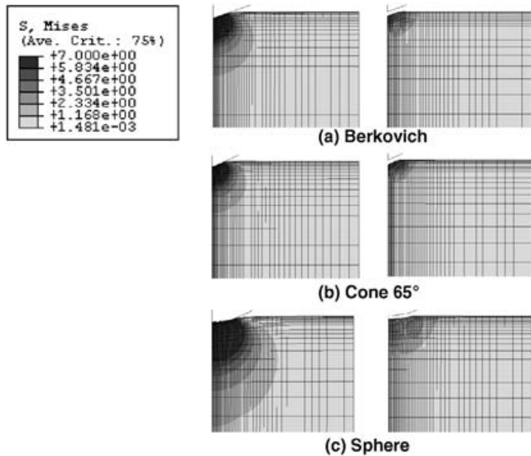

Fig. 6 Von-mises stress distribution for different tip shape (silicon)

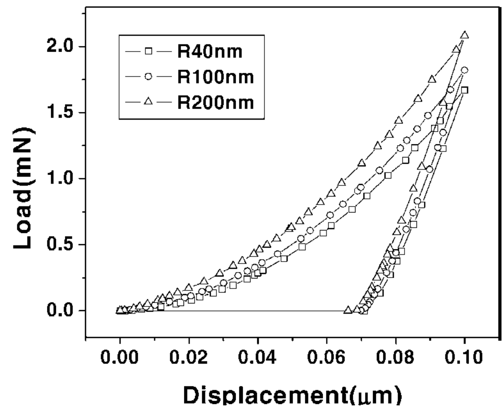

Fig. 7 Load-Displacement curves on silicon with different tip radius

the use of different indenters is different even if the same external force is applied, with a higher stress being developed by the sharper indenter. This in turn will lead to a larger plastic zone size formed with sharper indenter due to the higher stress concentration exerted.

The width and depth of indent traces are determined by the penetration depth of the indenter. Therefore, in order to perform nanometer-scale machining, the penetration depth of the tip should be very small. A problem is that a practical indenter has a nonzero tip radius, which is actually a sphere with a given radius. Therefore, when the penetration depth is too small, the deformation behavior of material is strongly affected by the elastic contact between the tip edge and the surface. This not only influences the area-depth function of the indenter but also affects the deformation behavior of the materials during the indentation process. Indentation simulations were performed with three different radiuses, 40, 100, and 200 nm. As shown in Fig. 7, the calculated load-displacement curves were very similar to those by Lu and Bogy (1995), and showed the indentation-size effect (ISE) (Fischer-Cripps, 2002). For a given indentation depth, the applied load and elastic recovery increased with the tip radius due to the increase of the contact area. Generally speaking, the ISE means that hardness at a small depth is much reater than at greater depths. At very low indentation depths, many factors (indenter geometry, tip-radius, surface roughness, phase transformation of material, friction between indenter and surface, surface-localized cold-work hardening resulting from polishing, lack of measurements capabilities, oxides, chemical contamination, and indentation conditions such as loading rate and applied load) do not allow a correct interpretation of the data because they change the contact area in a variety of ways (Lu and Bogy, 1995 ; Oliver and Pharr, 1992 ; Fischer-Cripps, 2002). The result in Fig. 7 shows an ISE due to the bluntness of the tip.

3.3 Effects of the pattern pitch and the tip radius (multi-array tip)

Indentation simulations using the 2-array tip were performed by varying the distance between the tips (D=500, 1000, 2000 nm), as shown in Fig. 8 (penetration depth=100 nm). It was found that the height of the pile-up formed between two tips increased with decreasing the D. In the case of D=500 nm, it was found that the residual stress fields around the tips were overlapped, as shown in Fig. 9 (c). In addition, the height of the pile-up formed between two tips increased with increasing penetration depth, as shown in Fig. 10.

Figure 11 shows the variation of the maximum pile-up height with increasing tip radius. The maximum pile-up height increased with increasing tip radius.

Copyright (C) 2005 NuriMedia Co., Ltd.

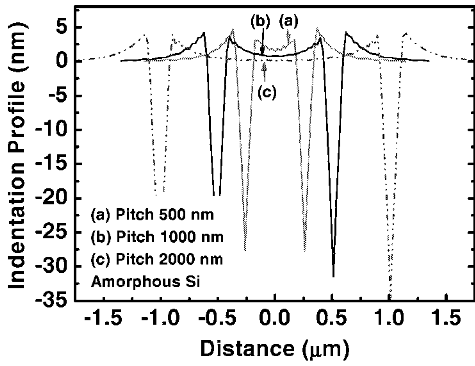

Fig. 8 Indentation profiles for different multi-tip width (D) after unloading

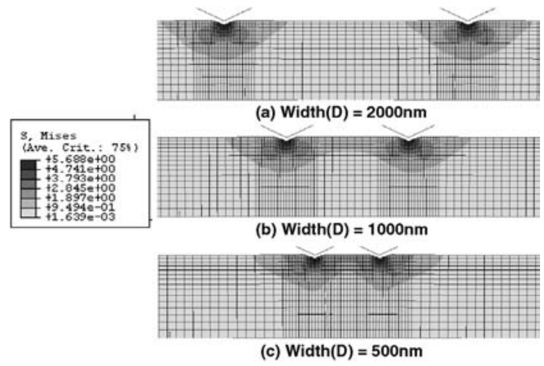

Fig. 9 Residual stress distribution for different multi-tip width (D) after unloading

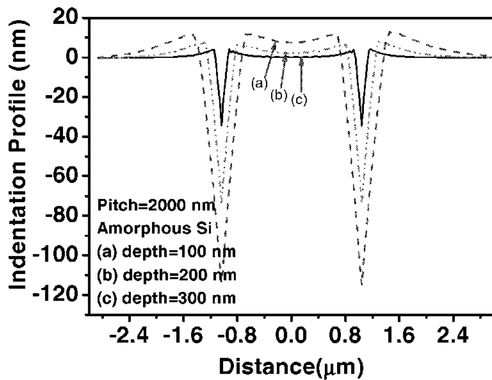

Fig. 10 Residual indentation profiles for different penetration depth after indentation with 2-array tips (D=2000 nm).

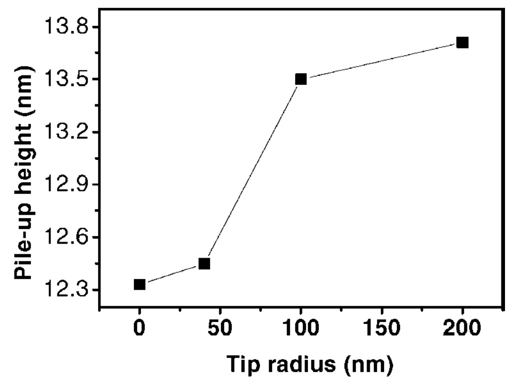

Fig. 11 Effect of tip radius on the maximum height of the pile-up formed between the tips

3.4 Effect of pattern pitch on the deformation behavior and etching characteristic of hard-brittle materials

In past studies, we have fabricated negative/positive pattern structures by a maskless fabrication technique using the combination of nano-scratch by nanoindenter and wet etching (Youn and Kang, 2004; 2005). In this study, we tried to investigate the effect of the pattern pitch on the deformation behavior and etching characteristic of hard-brittle materials, such as Si(100) and Pyrex 7740 glass.

Five grooves were machined on a Pyrex 7740 glass surface for variation of pitch of lines (Fig. 12). As shown in Fig. 12(b)-(d), the grooves with pitch of 2, 3, 4 μm show sound results with respect to the uniformity of line width and pitch. However, in the case of D=1 μm, the height of the region between two grooves was lower than the initial surface due to the effect of the sinking-in of adjacent groove.

Five grooves were machined on Si(100) surface with line pitch of 500 nm (Fig. 13). It was observed that the pattern region is higher than the initial surface due to the effect of the pile-up of adjacent grooves.

In order to investigate the effect of the pattern pitch on the final structure morphology after KOH etching, the groove pattern with the line pitch of 3 μm was fabricated on the Si(100) surface by the CLS process under different normal loads (L_n) of 1 and 5 mN (Fig. 14(a)), and it was etched in 20wt% KOH solutions for 20 min (Fig. 14(b)). Fig. 14(a) shows that the surface contacted by the tip protruded higher than the initial height of the surface and the protuberance

Copyright (C) 2005 NuriMedia Co., Ltd.

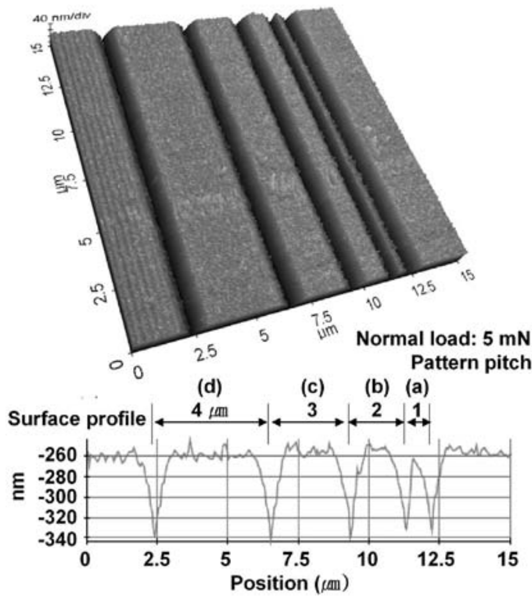

Fig. 12 AFM image and section profile of grooves on Pyrex 7740 surface machined by constant-load-scratch with different pitch ; (a) 1 (b) 2 (c) 3 and (d) 4 μm (normal load= 5 mN)

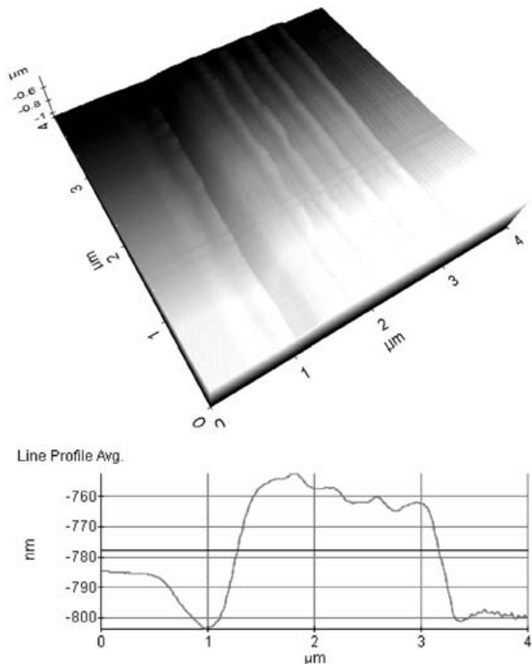

Fig. 13 AFM image and section profile of groove patterns on Si(100) surface with line pitch of 500 nm (normal load of 5 mN)

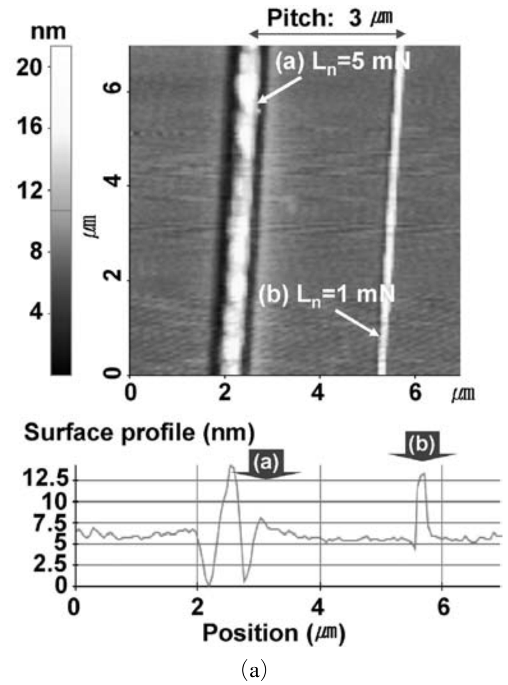

(a)

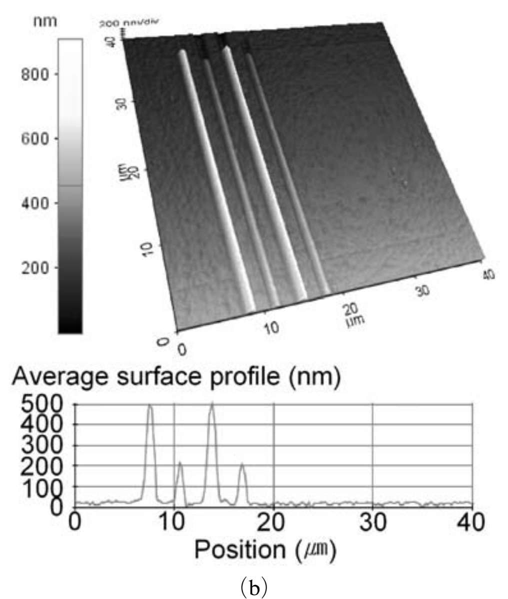

(b)

Fig. 14 The AFM image and the section profiles of line pattern with the line pitch of 2 μm (a) scratched under different normal load conditions (1 mN and 5 mN) and (b) after 20wt% KOH etching for 20 min

height increased with the increase of the normal load. It has been reported that the protuberance volume increases in accordance with the increase

Copyright (C) 2005 NuriMedia Co., Ltd.

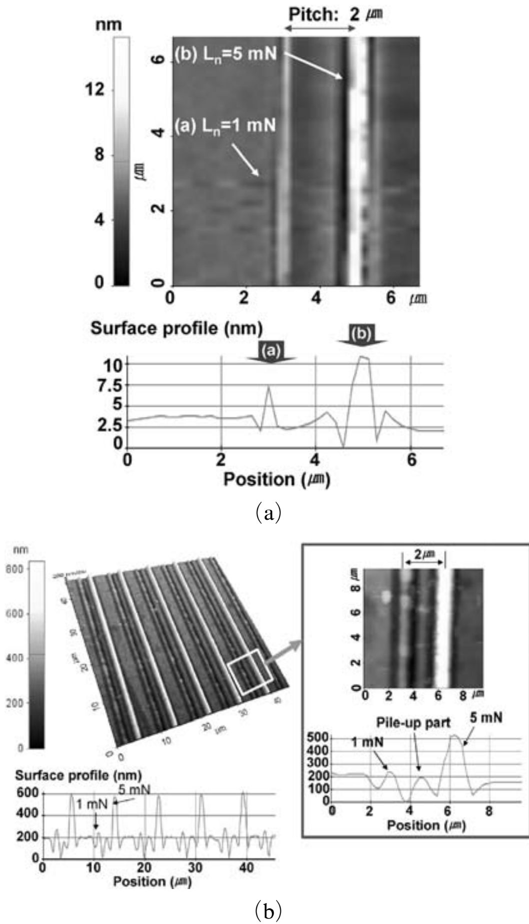

Fig. 15 The AFM image and the section profiles of line pattern with the line pitch of 2 ㎛ (a) scratched under different normal load conditions (1 mN and 5 mN) and (b) after 20wt% KOH etching for 20 min

of the normal load during a scratch experiment in atmosphere because the maximum tensile strength and shear strength that react on the scratched surface-the main cause of the breakage of the silicon combinations-increase with the increase of the normal load (Miyake and Kim, 2002 ; Youn and Kang, 2004). The positive-tone structure pattern with the line pitch of 3 ㎛ shows the sound results with respect to the uniformity of size and shape, as shown in Fig. 14(b). It is also shown that the size of positive-tone structure decreased with decreasing normal load. This indicates that the etch rate of scratched surface decreases with increasing applied normal load. It can be predicted that the scratched area became more stable compared to unscratched one and the stability of scratched area increase with increasing applied normal load.

The size and shape of the convex structures that were obtained after etching were also changed by varying etch-process conditions (KOH concentration, etch time, temperature, and others). The width of the convex structures was decreased with a decreasing normal load. The angle between the structure side wall and the (100) plane increased with increasing etching time due to the anisotropic etching properties of Si(100) material. It is well-known that the etch-stop plane of single crystal silicon in KOH solution is (111), and V-grooves are fabricated according to this fact in optical lithography technologies (Lang, 1996). Namely, if the angle between (100) and the etch plane becomes 54.7°, which value is the same as the angle between the (100) and the (100) plane, the etching rate is decreased to an insignificant degree.

Groove pattern with the line pitch of 2 ㎛ was fabricated by the CLS process under different normal loads (L_n) of 1 and 5 mN (Fig. 15(a)), and it was etched in 20wt% KOH solutions for 20 min (Fig. 15(b)). Unlike the result of Fig. 14 (b), the specimen with pitch of 2 ㎛ shows that the morphology of specimen surface is somewhat irregular due to both pile-up and residual stress field of material, as shown in Fig. 15(b).

4. Summary

In this study, the effects of tip-geometry factors (shape and tip radius) and process parameters (pattern pitch, normal load) on the deformation behaviors and etching characteristics of hard-brittle materials (Pyrex 7740 glass and silicon) were investigated by both experiment and FEM simulation.

(1) The effects of tip-geometry factors such as shapes (Berkovich, conical, spherical) and tip radii (40, 100, 200 nm) on the deformation behaviors of hard-brittle materials were investi-

Copyright (C) 2005 NuriMedia Co., Ltd.

gated by using finite element analysis. For a given depth, the applied load was the lowest in the case with conical indenter. In addition, the result for conical indenter showed the smallest elastic recovery. In addition, for a given depth, the applied load, the elastic recovery, and the area of the residual stress field increased with increasing the radius of tip.

(2) Indentation simulations using the two-array tip were performed by varying the distance between the tips (500, 1000, 2000 nm). It was found that the height of pile-up formed between two tips increased with decreasing the distance between tips. For a given pitch, the height of the pile-up formed between two tips increased with increasing the penetration depth and tip radius.

(3) Positive-tone structures were fabricated on Si(100) surface using the etch-mask effect of the scratched silicon surface. The positive-tone structure pattern with the line pitch of 3 μm shows the sound results with respect to the uniformity of size and shape. It is also shown that the size of positive-tone structure decreased with decreasing normal load. This indicates that the etch rate of scratched surface decreases with increasing applied normal load. Groove pattern with the line pitch of 2 μm that the morphology of specimen surface is somewhat irregular due to both pile-up and residual stress field of material.

Acknowledgments

This work was supported by National Research Laboratory (NRL) program of the Korean Ministry of Science and Technology (KMOST).

References

Ashida, K., Chen, L. and Morita, N., 2001, "New Maskless Micro-fabrication Technique of Single-crystal Silicon using the Combination of Nanometer-scale Machining and Wet Etching," in Proc. of 2nd euspen Int. Conf. 2001, Turin, Italy, May, pp. 78～81.

Blacley, W. S. and Scattergood, R. O., 1990, "Crystal Orientation Dependence of Machining Damage-A Stress Model," *Journal of the American Ceramic Society*, Vol. 73, Issue 10, pp. 3113～3115.

Chang, W. S., Shin, B. S. and Whang, K. H., 2003, "Nanoprobe Application Technologies," *Journal of KSPE*, Vol. 20, No. 3, pp. 5～14.

Chung, K. H., Lee, J. W. and Kim, D. E., 2004, "Nano-mechanical and Tribological Characteristics of Ultra Thin Amorphous Carbon Film Invested by AFM," *KSME International Journal*, Vol. 18, No. 10, pp. 1172～1781.

Fischer-Cripps, A. C., 2002, Nanoindenation (mechanical engineering series), Springer-Verlag (New York).

Hibbitt, Karlsson and Sorenson, 2001, ABAQUS Standard/Explicit rel. 6.2.

Lang, W., 1996, "Silicon Microstructuring Technology," *Materials Science and Engineering R*, Vol. R17, pp. 1～55.

Lu, C. J. and Bogy, D. B., 1995, "The Effect of Tip Radius on Nano-indenation Hardness Tests," *International Journal of Solids and Structures*. Vol. 32, No. 12, pp. 1759～1770.

Miyake, S. and Kim, J. D., 2002, "Increase and Decrease of Etching Rate of Silicon Due to Diamond Tip Sliding by Changing Scanning Density," *Japanese Journal of Applied Physics*, Vol. 41, pp. L1116～L1119.

Miyake, S. and Kim, J. D., 2001, "Fabrication of Silicon Utilizing Mechanochemical Local Oxidation by Diamond Tip Sliding," *Japanese Journal of Applied Physics*, Vol. 40, pp. L1247～L1249.

Morita, N., 2001, "Micro-fabrication Technique of Single Crystal Silicon by using Combination of Nano-scale Machining and Alkaline Etching," *Journal of the JSGE*, Vol. 45, No. 6, pp. 275～278.

Oliver, W. C. and Pharr, G. M., 1992, "An Improved Technique for Determining Hardness and Elastic Modulus using Load and Displacement Sensing Indentation Experiments," *Journal of Materials Research*, Vol. 7, pp. 1564～1583.

Shibata, T., Fuji, S., Makino, E. and Ikeda, M., 1996, "Ductile-regime Turning Mechanism of Single-crystal Silicon," *Journal of JSPE*, Vol. 18, No. 2/3, pp. 129～137.

Youn, S. W. and Kang, C. G., 2004, "Maskless

Copyright (C) 2005 NuriMedia Co., Ltd.

Pattern Fabrication on Si (100) Surface by using Nanoindenter with KOH Wet Etching," *Scripta Materialia*, Vol. 50, No. 1, pp. 105～109.

Youn, S. W. and Kang, C. G., 2005, "Etching Mask Effect of the Nanoscratched Borosilicate Surface and its Application to Maskless Pattern Fabrication," *Materials Science Forum*, Vols. 475-479, pp. 3479～3482.

Youn, S. W. and Kang, C. G., 2004, "Maskless Fabrication of the Silicon Stamper and its Application to the PDMS Casting Process," *Key Engineering Materials*, Vols. 274-276, pp. 445～450.

Youn, S. W. and Kang, C. G., 2004, "A Study on Nanoscratch Experiments of the Silicon and Borosilicate in Air," *Materials Science and Engineering A*, Vol. 384, pp. 275～283.

MTS Systems Corporation, 2002, Nanoindenter® XP manual.

Copyright (C) 2005 NuriMedia Co., Ltd.